Journal of Computational Methods in Molecular Design, 2013, 3 (4):11-21

Scholars Research Library
(http://scholarsresearchlibrary.com/archive.html)

ISSN : 2231- 3176
CODEN (USA): JCMMDA

Quantum-chemical modeling of the Hepatitis C Virus replicon inhibitory potency and cytotoxicity of some pyrido[2,3-*d*]pyrimidine analogues.

Ignacio Reyes-Díaz and Juan S. Gómez-Jeria*

Quantum Pharmacology Unit, Department of Chemistry, Faculty of Sciences, University of Chile, Las Palmeras 3425, Santiago 7800003, Chile

---

ABSTRACT

This paper uses a newly developed and extended formal quantum chemical method in an attempt to advance the knowledge of the relationship between the variation of several local atomic descriptors of the electronic structure of a set of pyrido[2,3-d]pyrimidine analogues and the variation of their inhibitory potencies in genotypes 1a and 1b hepatitis C virus (HCV) replicon assays and cytotoxicity in Huh-7 cells. Despite the lack of knowledge of the mechanism(s) of inhibition of the HCV replicons and of Huh-7 cell proliferation good quantitative structure-activity relationships (QSAR) were obtained for all biological activities studied. The equations relating structure and inhibitory capacity for 1a and 1b genotypes HCV replicons seem to be quite similar and involve mainly empty molecular orbitals localized on very specific atoms of the drugs. In the case of the cytotoxicity against Huh-7 cells the corresponding equation contains only contributions from occupied molecular orbitals localized on another set of specific atoms of the drugs. On the basis of our results a concrete atomic site is proposed as target to modify the biological activities.

Keywords: *Hepatitis C virus, Quantum Pharmacology, HCV replicons, structure-activity relationships.*

INTRODUCTION

Hepatitis C infection is a worldwide health problem affecting an estimated 170 million individuals. Chronic infection with hepatitis C virus (HCV) leads to liver fibrosis, cirrhosis and cancer. HCV is a small enveloped virus with a positive single-stranded RNA-genome of the family *Flaviviridae*. HCV has a wide variety of genotypes (at present with six major genotypes) [1-5]. Neither a vaccine against HCV nor an efficient therapy with a satisfactory broad spectrum of action against all genotypes of HCV is available. The research on hepatitis C and the development of new therapies have been slowed by the nonexistence of a permissive cell culture system supporting efficient replication of the virus. This problem has been surmounted in recent years [6-9].

Recently, Krueger et al. synthesized a group of pyrido[2,3-*d*]pyrimidine analogues and tested them for cytotoxicity in Huh-7 cells and inhibitory potency in genotype 1a and 1b HCV replicon assays [10]. The authors stated that "*in the absence of knowledge of the mechanism of inhibition and structural information on inhibitor binding, it is difficult to rationalize these results*". Here we present the results from a formal modeling of biological activities showing that, even if these *in vitro* effects are the final result of two or more unidentified or inadequately known processes, it is possible to provide solid quantitative structure-activity relationships for modeling the inhibitory potencies and cytotoxicity of these molecules.

MATERIALS AND METHODS

Methods, Models and Calculations

A formal way to obtain structure-activity relationships is based on the following philosophy. First, a model is proposed to explicate a specified biological activity. Next, by applying one or several physically-based approximations, the assumptions of the model are translated into one or more equations showing the expected relationships [11]. In our case, and starting from the statistical-mechanical definition of the equilibrium constant, we have continued to develop and enlarge a formal method relating the electronic structure of drugs to their *in vitro* receptor affinity constant [12-17]. In this way, good structure-activity relationships have been obtained for a variety of drugs and receptors [18-23]. The final result of this procedure is that, for the case of n molecules, we have the following system of n linear equations:

$$\log K_i = a + bM_{D_i} + c\log\left[\sigma_{D_i}/(ABC)^{1/2}\right] + \sum_j \left[e_j Q_j + f_j S_j^E + s_j S_j^N\right] +$$
$$+ \sum_j \sum_m \left[h_j(m)F_j(m) + x_j(m)S_j^E(m)\right] + \sum_j \sum_{m'} \left[r_j(m')F_j(m') + t_j(m')S_j^N(m')\right] +$$
$$+ \sum_j \left[g_j\mu_j + k_j\eta_j + o_j\omega_j + z_j\varsigma_j + w_j Q_j^{\max}\right] \quad (i=1,\ldots,n) \qquad (1)$$

where K_i is the drug-receptor affinity constant, M is the drug molecule's mass, σ its symmetry number, ABC the product of the drug molecule's moments of inertia about the three principal axes of rotation, Q_i is the net charge of atom i, S_i^E and S_i^N are, respectively, the total atomic electrophilic and nucleophilic superdelocalizabilities of Fukui et al., $F_{i,m}$ is the Fukui index (i.e., the electron population) of atom i in occupied (empty) MO (molecular orbital) m (m')[24]. $S_i^E(m)$ is the local atomic electrophilic superdelocalizability of atom i in occupied MO m, $S_i^E(m)$ is the local atomic nucleophilic superdelocalizability of atom i in empty MO m. The last bracket on the right side of Eq. 1 includes local atomic indices obtained by an approximate rearrangement of part of the remaining terms of the series expansion employed in the model [25]. μ_j, η_j, ω_j, ς_j and $Q_j^{\max}$ are, respectively, the local atomic electronic chemical potential of atom j, the local atomic hardness of atom j, the local atomic electrophilicity of atom j, the local atomic softness of atom j and the maximal amount of electronic charge that atom j may accept. Note that these new local atomic reactivity indices (LARIs) are expressed in the same units (eV) as the global ones and not in eV·e as are the usual projected local reactivity indices coming from Density Functional Theory (DFT) [25]. For example, the local atomic hardness of atom k, η_k, is defined as:

$$\eta_k = (E^*_{HOMO} - E^*_{LUMO}) \qquad (2)$$

where E^*_{HOMO} is the highest occupied molecular MO having a non-zero electron population on atom k and E^*_{LUMO} is the lowest empty MO having a non-zero (virtual) electron population on atom k. Then η_k is simply the local atomic $E^*_{HOMO} - E^*_{LUMO}$ gap that may or may not coincide with the molecular HOMO-LUMO gap (in fact, in the case of the hydrogen atoms within a molecule, their η_k values almost never coincide with the molecular HOMO-LUMO gap). In the following the symbol * makes reference to local atomic indices. S_i^E is related to the total electron-donating capacity of atom i and S_i^N to its total electron-accepting capacity. The local atomic Fukui indices and superdelocalizabilities are related to MO-MO interactions. μ_j is a measure of the tendency of an atom to gain or donate electrons: a large negative value indicates a good electron acceptor atom whereas a small negative value corresponds to a good electron donor atom. ω_i is related to the electrophilic power of an atom and includes the predisposition of the electrophilic atom to receive extra electronic charge together with its resistance to exchange charge with the medium. $Q_i^{\max}$ is the maximal amount of electronic charge that atom i may accept from another site. ς_j is defined as the inverse of the local atomic hardness of atom i [25-27].

Recently, we have expanded this model to analyze *in vitro* or *in vivo* biological activities other than drug-receptor equilibrium constants, with good results [27-29]. The basis of this expansion consists in accepting that all biological processes occurring, from the moment of the entry of a drug molecule into the biological system (*in vitro* or *in vivo*)

until the manifestation of any biological activity, are controlled by the same local atomic reactivity indices appearing in Eq. 1. It is important to note that this extended method is useful if and only if the whole set of molecules studied undergoes the same processes. The moment of inertia term can be expressed in a first approximation as:

$$\log\left[(ABC)^{-1/2}\right] \cong \sum_t \sum_t m_{i,t} R_{i,t}^2 = \sum_t O_t \qquad (3)$$

where the summation over t is over the different substituents of the molecule, $m_{i,t}$ is the mass of the i-th atom belonging to the t-th substituent, $R_{i,t}$ being its distance to the atom to which the substituent is attached. We have called these terms orientational parameters [17].

The selected molecules are shown in Table 1. Table 2 displays their corresponding inhibitory potencies in genotype 1a and 1b HCV replicon assays and their cytotoxicities in Huh-7 cells (a cell line of epithelial-like tumorigenic cells).

Table 1: Structures of pyrido[2,3-d]pyrimidine analogues

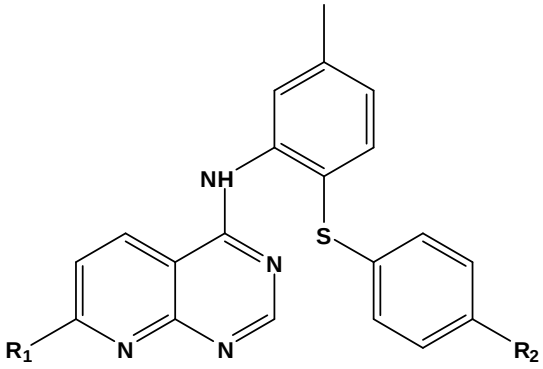

Molecule	R_1	R_2
1	Methyl	H
2	Methyl	OH
3	Methyl	OMe
4	Methyl	F
5	Methyl	H
6	Methyl	NHAc
7	Methyl	OH
8	1-Propyl	H
9	1-Propyl	NHAc
10	1-Propyl	OH
11	2-Propyl	H
12	2-Propyl	NHAc
13	2-Propyl	OH
14	2-Propyl	OMe
15	2-Propyl	F
16	2-Propyl	$NHSO_2Me$
17	Cyclopropyl	H
18	Cyclopropyl	NHAc
19	Cyclopropyl	OH
20	Cyclobutyl	H
21	Cyclobutyl	NHAc
22	Cyclobutyl	OH
23	*i*-Butyl	H
24	*i*-Butyl	NHAc
25	*i*-Butyl	OH
26	*t*-Butyl	OH
27	Cyclohexyl	OH

Table 2: Inhibitory potency in genotype 1a and 1b HCV replicon assays and cytotoxicity of molecules 1-27.

Compound	Replicon 1a log EC_{50} (µM)	Replicon 1b log EC_{50} (µM)	log *MTT* (µM)
1	1.12	0.58	1.35
2	1.37	-1.3	----
3	1.65	1.12	1.46
4	1.02	0.48	0.79
5	1.28	0.53	1.36
6	----	0.84	----
7	1.79	1	1.89
8	0.98	-0.49	1.07
9	1.14	-0.2	----
10	0.85	-0.6	1.49
11	1.01	0.53	0.9
12	0.41	1.14	1.46
13	-0.77	-1.8	1.36
14	1.06	0.23	0.94
15	0.51	0.26	0.68
16	1.28	1.05	----
17	1.02	0.57	1
18	1.18	0.23	1.47
19	1.02	0.2	1.24
20	0.79	0.2	0.56
21	1.2	0.57	1.69
22	1.05	0.49	1.5
23	1.12	0	0.88
24	1.44	0.52	1.58
25	1.16	0.28	1.05
26	0.66	-0.33	0.85
27	0.43	-0.06	----

We shall work within the common skeleton hypothesis that states that there is a certain group of atoms, common to all the molecules analyzed, that accounts for almost all the biological activities. The action of the substituents consists in modifying the electronic structure of this common skeleton and/or influencing the correct alignment of the drug through the orientational parameters. The common skeleton is shown in figure 1 together with the atom numbering employed in the resulting equations.

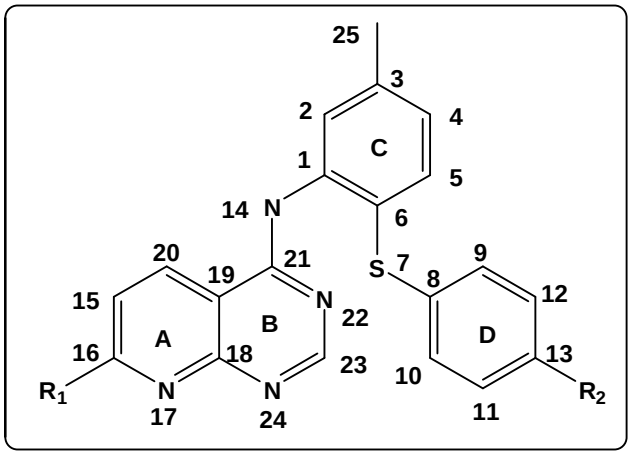

Figure 1. Common skeleton with atom numbering

Molecular geometries were fully optimized at the B3LYP/6-31G(d,p) level of theory with the Gaussian package [30]. From the corrected Mulliken Population Analysis results [31] we obtained numerical values for all electronic local atomic reactivity indices (LARIS) appearing in Eq. 1. Orientational parameters were calculated as usual [17, 20]. As the system of linear equations cannot be solved because the number of molecules is smaller than the number of unknown coefficients, linear multiple regression analyses (LMRA) were carried out separately for the each biological activity. The independent variables are the LARIS of all atoms of the common skeleton. For more details concerning the building of the matrix of independent variables see Refs. [23, 26, 27, 32, 33]. Here, statistics is used *not to see whether a structure-activity relationship exists, but to find the best one.*

RESULTS

For the genotype 1a HCV replicon assay results, preliminary and consecutive LMRAs showed that for molecules 9 and 26 the corresponding standard residual fell outside the ±2σ limit. Therefore these molecules were excluded from the final LMRA. The best equation obtained was:

$$\log(EC_{50}) = 1.38 - 13.31F_{25}(LUMO)^* - 4.42F_{11}(LUMO+2)^* + 2.46F_9(LUMO+2)^* + 0.80S^N_{20}(LUMO+1)^* + 0.04S^N_{12}(LUMO+2)^* + 0.15S^N_1(LUMO+1)^* - 8.97Q_2 \quad (4)$$

with n=24, R= 0.98, R²= 0.96, adj. R²= 0.94, F(7,16)=52.91 (p<0.00001), outliers>2σ=0 and SD= 0.12. Here, Q_2 is the net charge of atom 2, $S^N_1(LUMO+1)^*$ is the local atomic nucleophilic superdelocalizability of the second highest empty MO located on atom 1, $F_{25}(LUMO)^*$ is the Fukui index (i.e., the electronic population) of the first empty MO located on atom 25, and so on. There are no significant internal correlations between independent variables. Figure 2 shows the plot of observed values *vs.* calculated ones. The associated statistical parameters of Eq. 4 (Tables 3 and 4) show that this equation is statistically significant and that the variation of a group of local atomic reactivity indices belonging to the common skeleton explains about 96% of the variation of the inhibitory potency in the genotype 1a HCV replicon assay.

Table 3: The beta coefficients and *t*-test for the significance of coefficients of Eq. 4.

Variable	Beta	t(16)	p-level
$F_{25}(LUMO)^*$	-0.68	-11.60	0.000001
$F_{11}(LUMO+2)^*$	-1.05	-14.81	0.000001
$F_9(LUMO+2)^*$	0.62	8.85	0.000001
$S^N_{20}(LUMO+1)^*$	0.40	7.50	0.000001
$S^N_{12}(LUMO+2)^*$	0.39	6.54	0.000007
$S^N_1(LUMO+1)^*$	0.28	4.79	0.0002
Q_2	-0.20	-3.33	0.004

Table 4: Squared correlation coefficients for the variables appearing in Eq. 4.

	$F_{25}(LUMO)^*$	$F_{11}(LUMO+2)^*$	$F_9(LUMO+2)^*$	$S^N_{20}(LUMO+1)^*$	$S^N_{12}(LUMO+2)^*$	$S^N_1(LUMO+1)^*$
$F_{11}(LUMO+2)^*$	0.005	1.0				
$F_9(LUMO+2)^*$	0.17	0.28	1.0			
$S^N_{20}(LUMO+1)^*$	0.003	0.03	0.03	1.0		
$S^N_{12}(LUMO+2)^*$	0.02	0.16	0.03	0.002	1.0	
$S^N_1(LUMO+1)^*$	0.03	0.02	0.003	0.01	0.03	1.0
Q_2	0.04	0.0004	0.06	0.04	0.004	0.09

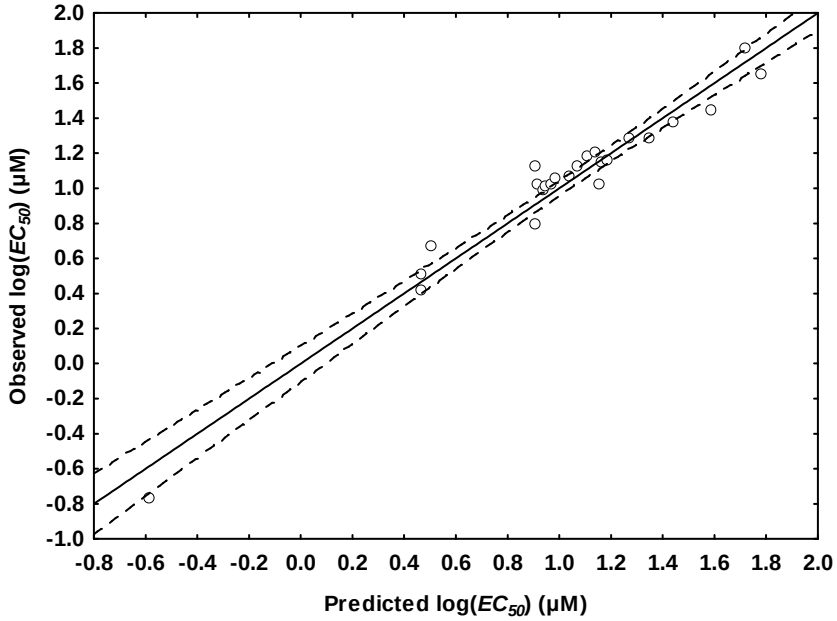

Figure 2. Plot of predicted *vs.* observed log(EC_{50}) values from Eq. 4. Dashed lines denote the 95% confidence interval.

For the genotype 1b HCV replicon assay results, a preliminary LMRA showed that for molecule 8 the corresponding standard residual fell outside the ±2σ limit. Therefore this molecule was excluded from the final LMRA. The best equation obtained was:

$$\begin{aligned}\log(EC_{50}) &= 3.21 - 11.49F_{25}(LUMO)^* - 17.92Q_{12} + 0.95F_3(HOMO-1)^* \\ &+0.40S_1^N(LUMO+1)^* + 0.03S_{24}^N(LUMO+2)^* - 0.64s_{11} \\ &-3.39F_{11}(LUMO+1)^* - 7.64F_{25}(LUMO+2)^*\end{aligned} \quad (5)$$

with n=26, R= 0.99, R^2= 0.97, adj. R^2= 0.96, F(8,17)=80.68 (p<0.00001), outliers>2σ=0 and SD= 0.13. Here, s_{11} is the softness of atom 11, Q_{12} is the net charge of atom 12, $F_k(MO_q)^*$ is the electron population of MO q located on atom k and $S_l^N(MO_p)^*$ is the local atomic nucleophilic superdelocalizability of atom l at empty MO p. There are no significant internal correlations between independent variables. Figure 3 shows the plot of observed values *vs.* calculated ones. The associated statistical parameters of Eq. 5 (Tables 5 and 6) show that this equation is statistically significant and that the variation of a group of local atomic reactivity indices belonging to the common skeleton explains about 96% of the variation of the inhibitory potency in genotype 1b HCV replicon assay.

Table 5: The beta coefficients and *t*-test for the significance of coefficients of Eq. 5.

Variable	Beta	t(17)	p-level
$F_{25}(LUMO)^*$	-0.45	-8.25	0.000001
Q_{12}	-0.39	-7.04	0.000002
$F_3(HOMO-1)^*$	0.22	4.54	0.0003
$S_1^N(LUMO+1)^*$	0.50	11.58	0.000001
$S_{24}^N(LUMO+2)^*$	0.45	7.88	0.000001
s_{11}	-0.19	-3.63	0.002
$F_{11}(LUMO+1)^*$	-0.60	-11.86	0.000001
$F_{25}(LUMO+2)^*$	-0.27	-5.68	0.00003

Table 6: Squared correlation coefficients for the variables appearing in Eq. 5.

	F_{25}(LUMO)*	Q_{12}	$F_3(HOMO-1)$*	$S_1^N(LUMO+1)$*	$S_{24}^N(LUMO+2)$*	S_{11}	$F_{11}(LUMO+1)$*
Q_{12}	0.01	1.0					
$F_3(HOMO-1)$*	0.02	0.03	1.0				
$S_1^N(LUMO+1)$*	0.04	0.005	0.04	1.0			
$S_{24}^N(LUMO+2)$*	0.08	0.005	0.18	0.002	1.0		
S_{11}	0.05	0.15	0.04	0.004	0.08	1.0	
$F_{11}(LUMO+1)$*	0.03	0.17	0.03	0.04	0.08	0.08	1.0
$F_{25}(LUMO+2)$*	0.02	0.0001	0.04	0.06	0.13	0.004	0.18

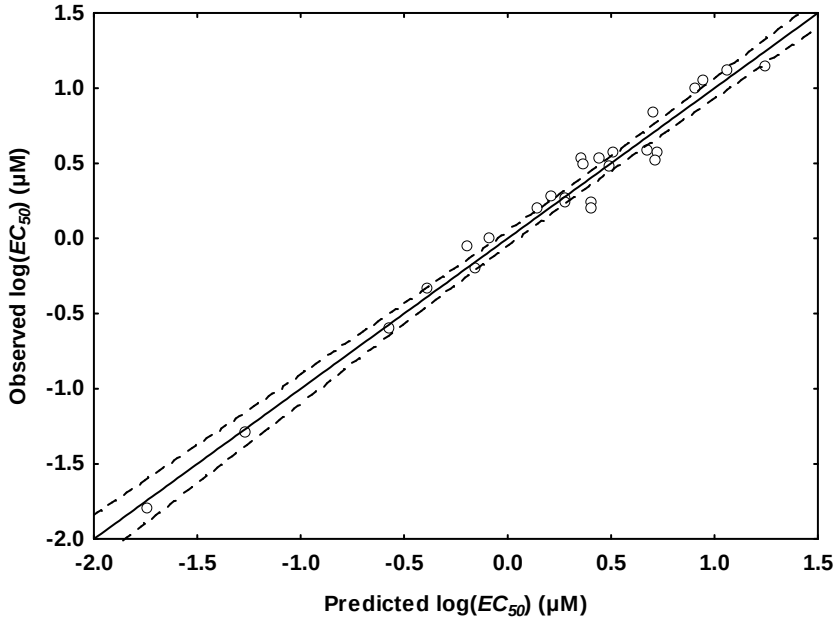

Figure 3. Plot of predicted *vs.* observed log(EC_{50}) values from Eq. 5. Dashed lines denote the 95% confidence interval.

For the cytotoxicity experimental results the best equation obtained was:

$$\log EC_{50} = 1.82 - 0.41F_{21}(HOMO-2)^* - 21.56F_{25}(HOMO-2)^* + 0.65S_{10}^E(HOMO-1)^* + 0.35S_{10}^E(HOMO-2)^* - 0.23S_{12}^E(HOMO-1)^* + 0.77F_{16}(HOMO-2)^* \quad (6)$$

with n=22, R= 0.97, R²= 0.94, adj. R²= 0.91, F(6,15)=36.83 (p<0.00001), outliers>2σ=0 and SD= 0.11. Here, $S_p^E(MO_t)^*$ is the local atomic electrophilic superdelocalizability of atom p at local occupied MO t and $F_k(MO_q)^*$ is the electron population of local MO q located on atom k. There are no significant internal correlations between independent variables. Figure 4 shows the plot of observed values *vs.* calculated ones. The associated statistical parameters of Eq. 6 (Tables 5 and 6) show that this equation is statistically significant and that the variation of a group of local atomic reactivity indices belonging to the common skeleton explains about 91% of the variation of the cytotoxicity in Huh-7 cells.

Table 7: The beta coefficients and *t*-test for the significance of coefficients of Eq. 6.

Variable	Beta	t(15)	p-level
F_{21}(HOMO-2)*	0.06	0.65	0.53
F_{25}(HOMO-2)*	-0.51	-6.99	0.000004
S^E_{10}(HOMO-1)*	0.88	8.66	0.000001
S^E_{10}(HOMO-2)*	0.75	7.62	0.000002
S^E_{12}(HOMO-1)*	-0.43	-4.65	0.0003
F_{16}(HOMO-2)*	0.26	3.78	0.002

Table 8: Squared correlation coefficients for the variables appearing in Eq. 6.

	F_{21}(HOMO-2)*	F_{25}(HOMO-2)*	S^E_{10}(HOMO-1)*	S^E_{10}(HOMO-2)*	S^E_{12}(HOMO-1)*
F_{25}(HOMO-2)*	0.0004	1.0			
S^E_{10}(HOMO-1)*	0.08	0.03	1.0		
S^E_{10}(HOMO-2)*	0.27	0.02	0.05	1.0	
S^E_{12}(HOMO-1)*	0.04	0.07	0.24	0.04	1.0
F_{16}(HOMO-2)*	0.002	0.01	0.02	0.02	0.02

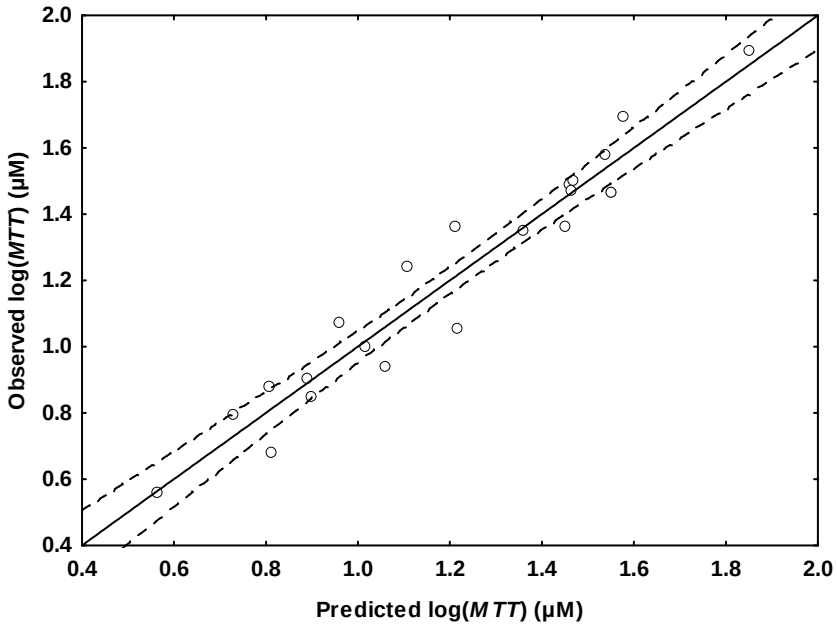

Figure 4. Plot of predicted *vs.* observed log(*MTT*) values from Eq. 6. Dashed lines denote the 95% confidence interval.

DISCUSSION

A variable-by-variable analysis [23, 27] of Eq. 4 indicates that a good inhibitory potency of the genotype 1a HCV replicon is associated with high values for $F_{25}(LUMO)^*$, $F_{11}(LUMO+2)^*$, $S^N_{20}(LUMO+1)^*$, $S^N_{12}(LUMO+2)^*$ and $S^N_1(LUMO+1)^*$, with a positive net charge on atom 2 and with a low value for $F_9(LUMO+2)^*$. Let us examine the variables associated with ring D (Fig. 1). Given that the local (LUMO+2)* of atoms 11 and 12 is of π nature we suggest that these atoms are acting as electron acceptors through (LUMO)*, (LUMO+1)* and (LUMO+2)* (all of π nature) in a π-π MO-MO interaction. As the local (LUMO+2)* of atom 9 is of σ nature and the $F_9(LUMO+2)^*$ value must be low, we suggest that atom 9 faces an electron donor center creating a repulsive MO-MO interaction that should be minimal in order to maximize the inhibitory activity. It is interesting to note that these three conditions are perfectly fulfilled at the same time if ring D interacts with a phenyl ring facing it. This is consistent with an alternating model of a conjugated aromatic phenyl ring. Regarding ring C, the fact that $F_{25}(LUMO)^*$ (for C-25, belonging to a methyl group) has σ nature and that this MO corresponds to the eighth highest empty molecular MO, suggests that the methyl group is facing an apolar area. This fact is consistent with the high local atomic hardness value for this atom (0.29 eV) compared, for example, with the local atomic hardness value for C-3 (0.15 eV). Atom 2 should have a positive net charge for optimal activity, indicating the possible presence of a negatively charged site. The high value required for $S^N_1(LUMO+1)^*$, a π MO, indicates that this atom acts as an electron acceptor through its (LUMO)* and (LUMO+1)*. The same reasoning holds for atom 20 of ring A. In the cases of atoms 1 and 20 we do not have enough information to allow us to clarify the exact nature of the complementary sites of interaction (i.e., aromatic rings, π MOs located on carbonyl groups, etc.). Finally, it is interesting to notice that in Eq. 4 only empty molecular orbitals appear. Note that only a few points lie just outside the 95% confidence limit in Fig. 2. This is a good indication that the common skeleton hypothesis works well for this case. All the above suggestions are summarized in the two-dimensional (2D) pharmacophore shown in Fig. 5.

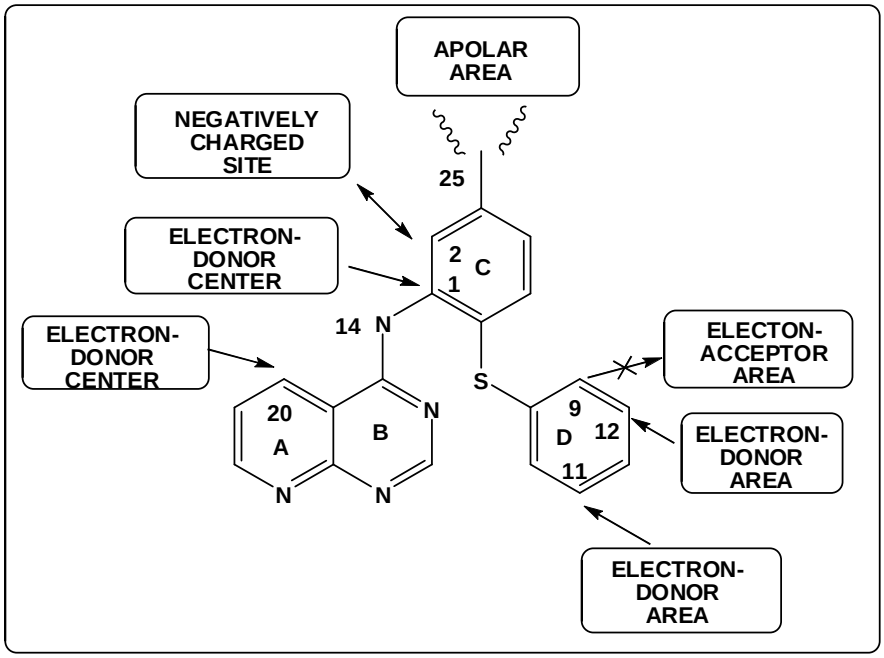

Figure 5. Partial 2D pharmacophore for the inhibitory potency on the genotype 1a HCV replicon

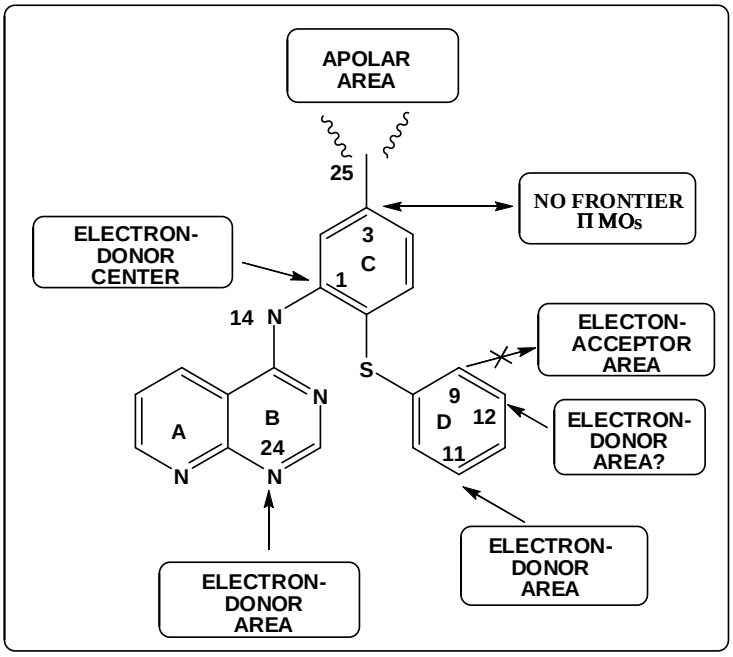

Figure 6. Partial 2D pharmacophore for the inhibitory potency on the genotype 1b HCV replicon

A variable-by-variable analysis of Eq. 5 indicates that a good inhibitory potency of the genotype 1b HCV replicon is associated with high values for $F_{25}(LUMO)^*$, $S_1^N(LUMO+1)^*$, $S_{24}^N(LUMO+2)^*$, $F_{11}(LUMO+1)^*$ and $F_{25}(LUMO+2)^*$; with a positive net charge on atom 12, a small value for $F_3(HOMO-1)^*$ and a high value for the local atomic softness of atom 11 (s_{11}). Regarding variables associated with ring D (Fig. 1), the situation is similar to the genotype 1a HCV replicon case. Atom 11 acts as an electron donor site through $F_{11}(LUMO)^*$ and $F_{11}(LUMO+1)^*$. This is reinforced by the requirement of a high value for the local softness s_{11}, which physically means that the local (HOMO)*-(LUMO)* gap for atom 11 should be small. A positive net charge on atom 12 suggests that this atom faces a negatively charged site and probably acts as an

electron acceptor. Notice that in the case of the genotype 1a HCV replicon case, atom 12 is also acting as an electron acceptor site. In the case of ring C we find that, as the local (LUMO)*, (LUMO+1)* and (LUMO+2) are of σ character, C-25 (belonging to a methyl group) should be interacting with an apolar area. The local (HOMO-1)* of atom 3 is a π orbital. A low value required for $F_3(HOMO-1)*$ might be considered a complementary requirement for the interaction of C-25 with the apolar area in the sense that an absence of highly polarizable electron densities favors that kind of interactions. Ring B participates in the process through atom 24, for which a high value of $S_{24}^{N}(LUMO+2)*$ is required. Knowing that the local MOs (LUMO)*, (LUMO+1)* and (LUMO+2)* of atom 24 are of π character, this atom should be interacting with an electron donor center of π nature. We do not have sufficient information to discern if atom 24 interacts alone or if part of ring B is involved in such a π-π interaction. Note that few points lie just outside the 95% confidence limit in Fig. 3. This is a good indication that the common skeleton hypothesis works well for this case too. Despite the fact that Eqns. 4 and 5 seem to be very similar, there is no linear relationship between the experimental values of $\log(EC_{50})$ for genotype 1a and 1b HCV replicon inhibition. All the above suggestions are summarized in the two-dimensional (2D) pharmacophore shown in Fig. 6.

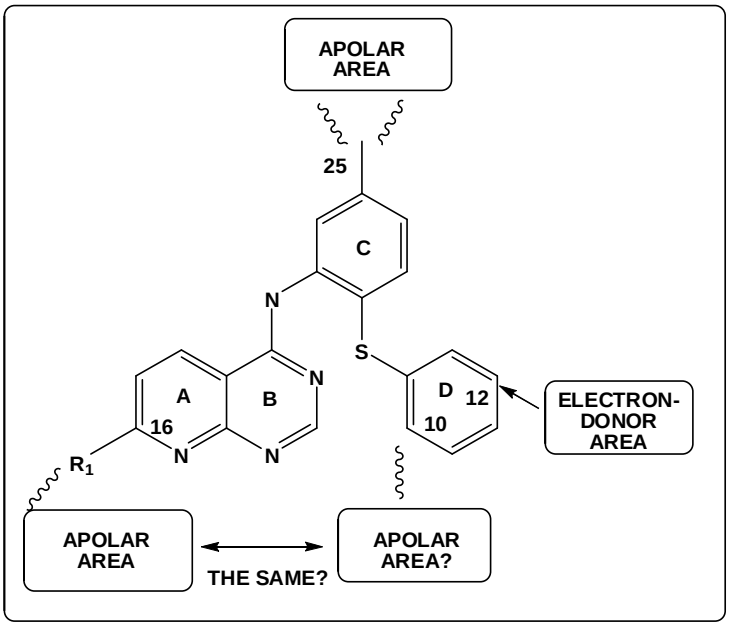

Figure 7. Partial 2D pharmacophore for cytotoxicity in Huh-7 cells.

Concerning cytotoxicity, note that several points are outside the 95% confidence limit in Fig. 4. This indicates that the common skeleton hypothesis does not work very well for the case of cytotoxicity. This fact suggests that we might be in the presence of extra interactions through the substituents of the common skeleton. We have found analogous dispersions of points in the analysis of indole-based reversible inhibitors of Hepatitis C virus NS5B polymerase [33] and antiproliferative activity of 1-azabenzanthrone derivatives in normal human fibroblasts [27]. For this reason, and considering the results of the *t*-test for the significance of coefficients of Eq. 6, we shall not discuss the $F_{21}(HOMO-2)*$ local reactivity index. The first fact to note is that all the process leading to cytotoxicity is related only to occupied MOs localized at very specific atoms. Low cytotoxicity is associated with high values of $\log(EC_{50})$. From Eq. 6 an optimal value for $\log(EC_{50})$ is associated with low values for $F_{25}(HOMO-2)*$, $S_{10}^{E}(HOMO-1)*$ and $S_{10}^{E}(HOMO-2)*$; and with high values for $S_{12}^{E}(HOMO-1)*$ and $F_{16}(HOMO-2)*$. In ring A the local (HOMO)* localized on atom 16 must have a high electron population (Fig. 1). Given that this MO is of σ nature we suggest that the R_1 substituent is facing an apolar area. The situation seems to be analogous for the case of C-25 on ring C. In the case of ring D local atomic reactivity indices associated with atom 10 appear twice. The requirements are that the electron donor capacities of the local (HOMO-1)* and (HOMO-2) MOs, both of π character, be low. Considering that the local (HOMO)* of atom 10 is of σ nature we may hypothesize that atom 10 faces an apolar area or one or more atoms with high

hardness and local σ MOs. A high value of $S_{12}^{E}(HOMO-1)*$, a π MO, suggests that atom 12 acts as an electron donor. All these suggestions are depicted in the 2D cytotoxicity pharmacophore for Huh-7 cells in Fig. 7.

In conclusion, despite the almost total lack of knowledge regarding the mechanisms of inhibition of the HCV replicons and of Huh-7 cell proliferation, we have been able to obtain solid and good quality structure-activity relationships for the molecules and biological activities studied here. This information should be useful for modulating together the whole process leading to low cytotoxicity and high inhibitory activity. It is noteworthy that the interaction of C-25 with apolar areas appears in all the statistical equations. Therefore, we suggest that substitution of the C-25 methyl group by other alkyl groups is a concrete way that should be explored by experimental medicinal chemists.

REFERENCES

[1]DN Fusco; RT Chung, *Ann. Rev. Med.*, **2012**, 63 (1), 373.
[2]LW Meredith; GK Wilson; NF Fletcher; JA McKeating, *Rev. Med. Virol.*, **2012**, 22 (3), 182.
[3]R Bartenschlager; V Lohmann; F Penin, *Nat. Rev. Microbiol.*, **2013**, 11 (7), 482.
[4]M Gu; CM Rice, *Curr. Opin. Virol.*, **2013**, 3 (2), 129.
[5]TKH Scheel; CM Rice, *Nat. Med.*, **2013**, 19 (7), 837.
[6]V Lohmann; F Körner; J-O Koch; U Herian; L Theilmann; R Bartenschlager, *Science*, **1999**, 285 (5424), 110.
[7]R Bartenschlager; V Lohmann, *J. Gen. Virol.*, **2000**, 81 (7), 1631.
[8]KJ Blight; AA Kolykhalov; CM Rice, *Science*, **2000**, 290 (5498), 1972.
[9]M Ikeda; M Yi; K Li; SM Lemon, *J. Virol.*, **2002**, 76 (6), 2997.
[10] A Chris Krueger; DL Madigan; DW Beno; DA Betebenner; R Carrick; BE Green; W He; D Liu; CJ Maring; KF McDaniel; H Mo; A Molla; CE Motter; TJ Pilot-Matias; MD Tufano; DJ Kempf, *Bioorg. Med. Chem. Lett.*, **2012**, 22 (6), 2212.
[11] YC Martin, *Quantitative drug design : a critical introduction*, M. Dekker, New York, 1978.
[12] D Agin; L Hersh; D Holtzman, *Proc. Natl. Acad. Sci.* (USA), **1965**, 53 (5), 952.
[13] F Peradejordi; AN Martin; A Cammarata, *J. Pharm. Sci.*, **1971**, 60 (4), 576.
[14] F Tomas; JM Aulló, *J. Pharm. Sci.*, **1979**, 68 (6), 772.
[15] JS Gómez-Jeria, *Int. J. Quant. Chem.*, **1983**, 23 (6), 1969.
[16] JS Gómez-Jeria, "Modeling the Drug-Receptor Interaction in Quantum Pharmacology," in *Molecules in Physics, Chemistry, and Biology*, J. Maruani Ed., vol. 4, pp. 215, Springer Netherlands, **1989**.
[17] JS Gómez-Jeria; M Ojeda-Vergara, *J. Chil. Chem. Soc.*, **2003**, 48 (4), 119.
[18] JS Gómez-Jeria; DR Morales-Lagos, *J. Pharm. Sci*., **1984**, 73 (12), 1725.
[19] JS Gómez-Jeria; D Morales-Lagos; BK Cassels; JC Saavedra-Aguilar, *Quant. Struct.-Relat.*, **1986**, 5 (4), 153.
[20] JS Gómez-Jeria; M Ojeda-Vergara; C Donoso-Espinoza, *Mol. Engn.*, **1995**, 5 (4), 391.
[21] JS Gómez-Jeria; L Lagos-Arancibia; E Sobarzo-Sánchez, *Bol. Soc. Chil. Quím*., **2003**, 48 (1), 61.
[22] JS Gómez-Jeria, *J. Chil. Chem. Soc*., **2010**, 55 (3), 381.
[23] F Salgado-Valdés; JS Gómez-Jeria, *J. Quant. Chem.*, **2013**, in press.
[24] K Fukui; H Fujimoto, *Frontier orbitals and reaction paths: selected papers of Kenichi Fukui*, World Scientific, Singapore; River Edge, N.J., **1997**.
[25] JS Gómez-Jeria, *Canad. Chem. Trans.*, **2013**, 1 (1), 25.
[26] JS Gómez-Jeria, *Elements of Molecular Electronic Pharmacology (in Spanish)*, Ediciones Sokar, Santiago de Chile, 2013.
[27] JS Gómez-Jeria; M Flores-Catalán, *Canad. Chem. Trans*., **2013**, 1 (3), 215.
[28] C Barahona-Urbina; S Nuñez-Gonzalez; JS Gómez-Jeria, *J. Chil. Chem. Soc*., **2012**, 57 (4), 1497.
[29] DA Alarcón; F Gatica-Díaz; JS Gómez-Jeria, *J. Chil. Chem. Soc.*, **2013**, 58 (3), 1651.
[30] MJ Frisch; GW Trucks; HB Schlegel et al., "Gaussian98 Rev. A.11.3," Gaussian, Pittsburgh, PA, USA, 2002.
[31] JS Gómez-Jeria, *J. Chil. Chem. Soc*., **2009**, 54 (4), 482.
[32] T Bruna-Larenas; JS Gómez-Jeria, *Int. J. Med. Chem.*, **2012**, 2012 Article ID 682495 (Article ID 682495), 1.
[33] A Paz de la Vega; DA Alarcón; JS Gómez-Jeria, *J. Chil. Chem. Soc*., **2013**, Accepted for publication.